Enhanced thermal stability and spin-lattice relaxation rate of N@C_{60} inside carbon nanotubes

S. Tóth,[1] D. Quintavalle,[1] B. Náfrádi,[2] L. Korecz,[3] L. Forró,[2] and F. Simon[1,*]

[1]*Budapest University of Technology and Economics, Institute of Physics and Condensed Matter Research Group of the Hungarian Academy of Sciences, H-1521, Budapest P.O. Box 91, Hungary*

[2]*Institute of Physics of Complex Matter, FBS Swiss Federal Institute of Technology (EPFL), CH-1015 Lausanne, Switzerland and*

[3]*Chemical Research Center, Institute of Chemistry, P.O. Box 17, H-1525 Budapest, Hungary*

(Received 30 January 2008; revised manuscript received 18 March 2008; published 5 June 2008)

We studied the temperature stability of the endohedral fullerene molecule N@C_{60} inside single-wall carbon nanotubes using electron-spin-resonance spectroscopy. We found that the nitrogen escapes at higher temperatures in the encapsulated material as compared to its pristine, crystalline form. The temperature dependent spin-lattice relaxation time T_1 of the encapsulated molecule is significantly shorter than that of the crystalline material, which is explained by the interaction of the nitrogen spin with the host nanotubes.

DOI: 10.1103/PhysRevB.77.214409 PACS number(s): 73.63.Fg, 72.80.Rj, 76.30.−v

I. INTRODUCTION

Fullerenes encapsulated inside single-wall carbon nanotubes (SWCNTs)[1,2] is an interesting molecular nanostructure as it combines two fundamental forms of carbon. The existence of this so-called peapod structure[3] inspired a number of fundamental and application oriented studies. The growth of peapods was studied with molecular dynamics simulations[4] and the existence of the structure was explained by the net energy gain per encapsulated fullerenes.[5–8]

An intriguing class of peapods is that with encapsulated magnetic fullerenes such as metallofullerenes,[9] the endohedral N@C_{60},[10] and C_{59}N.[11] Peapods with magnetic fullerenes can be used to study the electronic properties of the tubes[11] and may be suitable for quantum information processing[12,13] and they are candidates for magnetic force microscopy cantilevers. The N@C_{60} fullerene is a unique molecule as it contains an atomic nitrogen with the $S=3/2$ spin configuration.[14] The atomic nitrogen weakly interacts with its environment resulting in long electron-spin-lattice relaxation times T_1s.[15] However, the N@C_{60} molecule is sensitive to temperature and annealing to ~500 K irreversibly destroys it through the escape of the nitrogen.[16] This motivated us to study the thermal stability of N@C_{60} when it is encapsulated inside SWCNTs. The modification of the electronic state of the molecule upon encapsulation is also of interest as it can yield information about the fullerene-tube interaction and about the electronic structure of the nanotubes.

Here, we report on high-temperature electron-spin-resonance (ESR) spectroscopy on the encapsulated N@C_{60}. We find that the molecule decays much slower than its pristine counterpart in the crystalline form, which indicates that the presence of the nanotubes stabilize the molecule. T_1 of N@C_{60} in the peapod form is significantly shorter than in the crystalline form.

II. EXPERIMENT

We prepared peapods from commercial purified SWCNTs (Nanocarblab, Moscow, Russia, purity 50 wt %) and N@C_{60}:C_{60} fullerenes with a 400 ppm N@C_{60}. The endohedral fullerene was produced by the N implantation method[14] purified and concentrated by chromatography. A suspension of SWCNT in toluene containing dissolved N@C_{60}:C_{60} was sonicated for 2 h, filtered with a 0.4 micron pore size filter and dried at room temperature. Electron microscopy, Raman and electron-energy-loss spectroscopies, and x-ray diffraction studies indicate that sizable filling can be obtained with similar solvent methods.[10,17] The samples were ground to enable penetration of the exciting microwaves. In the following, we refer to the starting N@C_{60}:C_{60} as "crystalline" and to the encapsulated material as "peapod." Both kinds of samples were sealed in quartz tubes under He atmosphere. Experiments were carried out using an Elexsys E500 spectrometer with a TE011 cavity equipped with gas-flow inserts. The ESR signal intensity, which is proportional to the number of spins observed, was determined by fitting Lorentzian curves to the data.

III. RESULTS AND DISCUSSION

The ESR spectra of the crystalline and peapod N@C_{60}:C_{60} materials are shown for different temperatures in Fig. 1. A triplet signal, which is characteristic for the hyperfine interaction of the N spins with the ^{14}N nucleus with nuclear spin $I=1$ is observed for both kinds of samples. The three unpaired electrons on the $2p^3$ nitrogen atomic orbitals are in a high spin, $S=3/2$ state configuration. The zero-field splitting of the electron Zeeman levels is small due to the high symmetry of the fullerene cage and it can be observed in spin-echo ESR experiments only.[18] The isotropic nuclear hyperfine coupling, $A_{iso}=0.565$ mT of N@C_{60} is uniquely large due to the compression of the nitrogen orbitals, which unambiguously identifies the observation of this molecule.[14]

Besides the triplet, the peapod spectra contains a broad background (not shown) due to the inevitable presence of ferromagnetic Ni:Y catalysts in the SWCNT samples. However, the peapod spectrum does not contain any impurity line around $g=2$ as observed in the early studies,[10,19] which attests the high SWCNT sample purity. The ESR signal intensity observed for the peapod sample was compared to that in the crystalline sample, which enables to determine the amount of N@C_{60} in the peapods. We found that fullerene

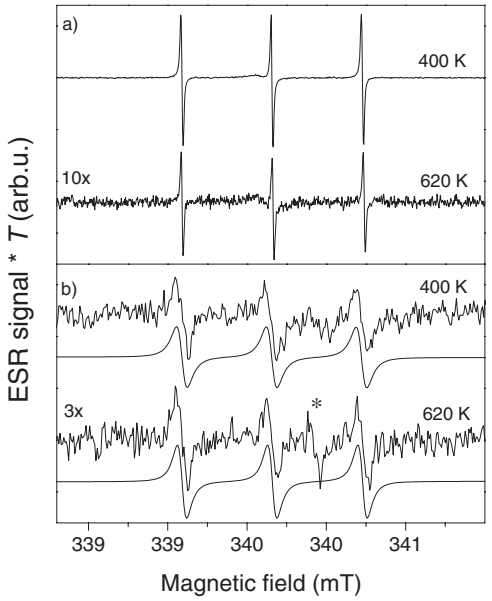

FIG. 1. ESR spectra of the crystalline (a) and peapod (b) $N@C_{60}:C_{60}$ multiplied by the temperature. The data are shown on different scales for the two kinds of materials. Note the magnified vertical scale for the high-temperature data. Solid curves are fit to the data. Asterisk indicates an impurity signal from the quartz tube.

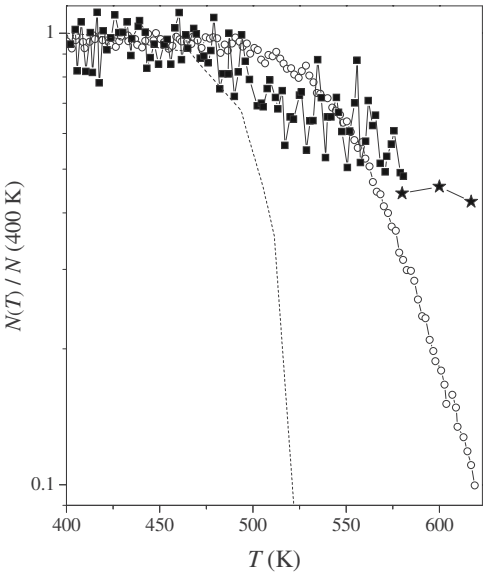

FIG. 2. Temperature dependence of the number of $N@C_{60}$ spins, $N(T)$ normalized to the 400 K values, ○: crystalline, ■: peapod. The longer averaged data for the peapod material at 580, 600, and 620 K are shown with asterisks. Dashed curve shows similar measurements on the crystalline material from Ref. 16. Note the logarithmic vertical scale.

content in the peapod is ~2–3 wt %, in agreement with the previous studies.[10,20]

The number of $N@C_{60}$ spins, $N(T)$, is proportional to the product of the ESR signal intensity and the temperature as the magnetic susceptibility of the $N@C_{60}$ spins follows a Curie temperature dependence. Since we are interested in the change of $N(T)$ as a function of temperature, normalizing it to a well defined temperature value allows a precise monitoring of the decay of $N@C_{60}$. In Fig. 2, we show the temperature dependence of the number of $N@C_{60}$ spins in both kinds of samples normalized to the value at 400 K. For comparison, we show the corresponding data from Ref. 16. The annealing speed was 90 s/2 K, that is identical to the heating protocol used in Ref. 16. At 580, 600, and 620 K, we performed longer data acquisition, thus less temperature points were taken to maintain the annealing protocol. We observe a clear drop in the number of $N@C_{60}$ for the crystalline material when heated above ~550 K. However, we observe that the decay is less sharp and that it occurs at about 50 K, higher temperature than that observed previously.[16] We have no clear explanation for this difference between ours and the previous studies. We carefully checked our thermometry and we used a large flux of exchange gas. In addition, *ex situ* annealing, i.e., heating both samples outside the ESR cavity in a furnace while approximately following the above annealing protocol, gave identical decay curves as the *in situ* result.

The important observation is that the number of $N@C_{60}$ does not decay in the peapod sample as fast as in the crystalline material. We observe about relatively three times as much $N@C_{60}$ in the peapod material at 620 K than in the crystalline material. This effect is also apparent in Fig. 1 where the corresponding spectra are shown. Although the noise in the peapod data limits the conclusions, the decay of $N@C_{60}$ appears to start already at 500 K but there is no sharp decay such as that observed for the crystalline material. The amount of $N@C_{60}$ decreases rather smoothly with increasing temperature, however, we could not follow this above 620 K due to technical limitations.

In the following, we discuss the origin of the enhanced thermal stability of $N@C_{60}$ inside nanotubes. It was proposed in Ref. 16 that the atomic nitrogen escapes from the fullerene cage by forming bonds with two neighboring carbon atoms from the inside and by swinging through the bonds to the outside of the fullerene. This was supported by the observation of enhanced stability of the encaged nitrogen when the fullerene was functionalized, which effectively suppresses the probability of this escape path. *Ab initio* electronic structure calculations on the peapods indicate a hybridization of the orbitals on the fullerenes and the nanotubes.[8] Raman spectroscopy on the peapods provided experimental evidence for hybridization and a partial charge transfer between the nanotubes and the fullerenes.[21] We suggest that these effects suppress the inside-the-cage bond formation for the peapod $N@C_{60}$ similar to functionalization of the molecules.

In addition to the modified electronic structure of fullerenes, the peapod geometry may also play a role in the enhanced thermal stability of $N@C_{60}$. The one-dimensional lattice constant of fullerenes inside the tubes is 0.97 nm (Ref. 22) that is about half way between the 1.002 nm fullerene-fullerene spacing in crystalline C_{60} (Ref. 23) and 0.961 nm for polymerized *fcc* C_{60}.[24] This probably limits the above described escape process of nitrogen simply by geometrically limiting the available room for the above described swinging-out process. For both mechanisms, the Gaussian

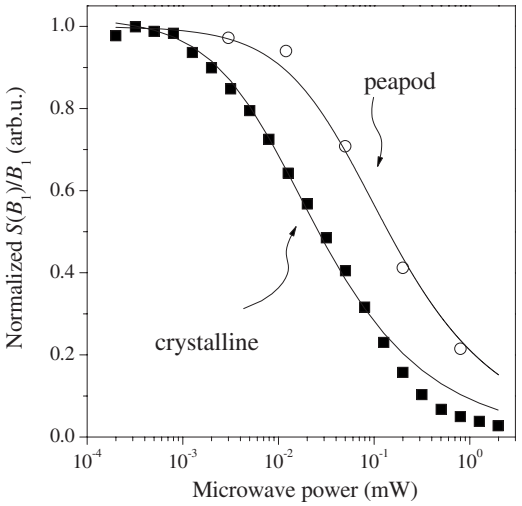

FIG. 3. Saturation curves of $N@C_{60}$ and peapod $N@C_{60}$ at 300 K. The ESR intensities are divided by the microwave magnetic field B_1 and are normalized to the values at the lowest power. Solid curves are calculated saturation curves with Eq. (1) and the parameters given in Table I. Note that the solid curve for the crystalline material is calculated with relaxation times determined in spin-echo measurements in Ref. 12 with no further adjustable parameters.

distribution of tube diameters with an average of 1.4 and 0.1 nm variance explains why the thermally induced decay of $N@C_{60}$ is spread out in temperature: we expect that both the electronic modification of the fullerenes through the fullerene-nanotube interaction and also the geometrical effect are strongly influenced by the diameter of the host tubes.

The spin-lattice relaxation time of a paramagnetic spin can be used to study the electronic structure of its environment. Well known example of this is the Korringa-relaxation, i.e., $1/T_1T=$const. of nuclear spins when these are embedded in metals.[25] In our case, the T_1 of encapsulated $N@C_{60}$ can be studied using saturated ESR measurement.[26] In this method, the ESR signal intensity, S is progressively saturated upon increasing microwave power and it follows:[25,26]

$$S(p) \propto \frac{\sqrt{p}}{\sqrt{1 + CQ\gamma^2 p T_1 T_2}} \tag{1}$$

where $\gamma_e/2\pi=28.0$ GHz/T is the electron gyromagnetic ratio, p is the microwave power, T_2 is the spin-spin relaxation time of the individual spin-packets. C is a constant that depends on the microwave cavity mode with quality factor Q and describes how large microwave magnetic field, $B_1 = \sqrt{CQp}$, is produced for a power of p. Taking into account that only one of the two circularly polarized magnetic-field components of the linearly polarized field is ESR active, we obtain for the TE011 cavity $C=2.2\cdot 10^{-12}$ T^2/W.[27] In Fig. 3, we show the saturated ESR results for the crystalline and the peapod material at 300 K.

Clearly, the ESR signal of the peapod material saturates at larger microwave powers, which indicates a shorter T_1 relaxation time. To obtain T_1 values from the saturation curves using Eq. (1), the value for T_2 has to be known. T_2 is the spin-spin relaxation time of individual spin-packets that is given by the dipolar interaction of like-spins provided T_1 is long enough and does not give a homogeneous broadening.[28] If this is the case, T_2 can be determined from the dipolar interaction strength of the like spins and is inversely proportional to their concentration. $T_2=5$ μs is obtained for the 400 ppm $N@C_{60}:C_{60}$ crystalline material from the $T_2=20$ μs for a 100 ppm $N@C_{60}:C_{60}$ sample.[12] As shown in Table I, is much longer for the crystalline material so no homogeneous broadening of the spin-packets occurs. This situation is reversed for the peapod material: the low concentration of the like nitrogen spins would give a long $T_2 \sim 250$ μs based on the $\sim 2\%$ fullerene weight percentage in the peapod. However, T_1 is shorter than that value, which gives a homogeneous broadening of the individual spin-packets and sets $T_1=T_2$. As we show below, this holds down to the lowest temperatures. It is interesting to note here that a similar situation was encountered for another diluted magnetic fullerene peapod system, the $C_{59}N:C_{60}$, where the rapid T_1 relaxation causes a homogeneous broadening.[11]

TABLE I. T_1 and T_2 at 300 for the crystalline and peapod materials used to calculate the saturated ESR data. We used the experimental quality factors of $Q=3000$ and 2000 for the crystalline and peapod materials, respectively. The $T_2=5$ μs of the crystalline material was obtained for our 400 ppm sample from the $T_2=20$ μs for a 100 ppm $N@C_{60}:C_{60}$ sample.

	T_1 [μs]	T_2 [μs]
crystalline (Ref. 12)	120	5
peapod	13	13

We show the simulated saturation curves in Fig. 3 with the parameters given in Table I. The excellent agreement for the measured and calculated saturation curves for the crystalline material shows that the saturated ESR measurement can be used to determine values for T_1 and T_2, although it lacks the direct access to these values such as the spin-echo ESR method. It thus justifies the use of the saturated ESR method to determine the T_1 and T_2 values for the peapod system as well.

We determined the temperature dependence of T_1 from the saturated ESR measurements in the 10–80 K temperature range in addition to the 300 K data. Measurements at other temperatures were hindered by spectrometer stability. We show the $1/T_1$ data in Fig. 4. for the peapod material. We also show the same data for the crystalline material from Ref. 15. The $1/T_1$ spin-lattice relaxation rate is roughly one order of magnitude larger for the peapod material than for the crystalline at room temperature. It is even larger at 10 K for the peapod than the corresponding value for the crystalline material. The temperature dependence of $1/T_1$ is also different for the two kinds of compounds: for the peapod it decreases with temperature to a residual value, whereas it vanishes exponentially for the crystalline material.[15] It was proposed in Ref. 15 that T_1 in crystalline $N@C_{60}$ is given by the quantum oscillator motion of the encaged nitrogen through the modulation of the hyperfine field, which results in the exponential freezing-out of the relaxation rate.

T_1 was measured for the $N@C_{60}$ peapods[19,29] and a distributed and about an order of magnitude shorter T_1 value

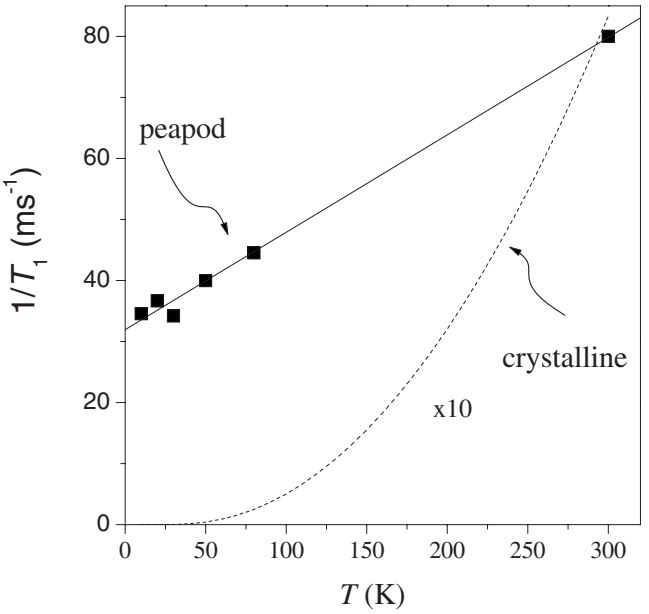

FIG. 4. Temperature dependence of the spin-lattice relaxation rate $1/T_1$ for peapod. We show the corresponding data for the crystalline material from Ref. 15 magnified by 10 with a dashed curve. Solid line is a guide to the eye.

was found than in the current study. We believe that the current, longer T_1 values better approach the intrinsic, i.e., less defect influenced T_1 of the peapod system. The enhanced relaxation rate in the peapod material is given by additional relaxation mechanisms. We expect that the hyperfine relaxation is not significantly different in the peapod material as the isotropic hyperfine coupling is unchanged. Possible mechanisms for the relaxation are coupling to conduction electrons on the tubes and paramagnetic relaxation from defects on the tubes and from the transition-metal catalyst particles, which are inevitably present in the nanotube samples. The latter relaxation mechanism could explain the presence of the residual relaxation rate as it is inversely proportional to the temperature.[28] This contribution is expected to be negligible at room temperature, therefore the factor 10 enhancement of the room-temperature relaxation rate for the peapod is suggested to originate from the coupling of the nitrogen spins to the conduction electrons on the tubes, i.e., from a Korringa relaxation. It is important to note here that we do not observe a multicomponent saturation, i.e., there seems to be a single T_1 time for the encapsulated $N@C_{60}$.

IV. CONCLUSIONS

In summary, the $N@C_{60}$ molecule is more stable in peapod than in crystalline form. This was suggested to result from the modified electronic structure of fullerenes inside the tubes and from the compact packing of the fullerenes. The spin-lattice relaxation time of the $N@C_{60}$ spins is much shorter in the peapod form and it remains finite at the lowest temperature. This puts severe limit on the applicability of the NC_{60} peapod system for quantum information processing.

ACKNOWLEDGMENTS

We thank A. Jánossy and A. Rockenbauer for stimulating discussions and K.-P. Dinse for the endohedral fullerenes. We acknowledge the Hungarian State Grants (OTKA) No. TS049881, No. F61733, No. NK60984, K72781, and T046953, the Swiss National Science Foundation, and the European research network IMPRESS.

*Corresponding author: ferenc.simon@univie.ac.at

[1] S. Iijima and T. Ichihashi, Nature (London) **363**, 603 (1993).
[2] D. S. Bethune, C. H. Kiang, M. S. De Vries, G. Gorman, R. Savoy, and R. Beyers, Nature (London) **363**, 605 (1993).
[3] B. W. Smith, M. Monthioux, and D. E. Luzzi, Nature (London) **396**, 323 (1998).
[4] S. Berber, Y.-K. Kwon, and D. Tománek, Phys. Rev. Lett. **88**, 185502 (2002).
[5] M. Melle-Franco, H. Kuzmany, and F. Zerbetto, J. Phys. Chem. B **107**, 6986 (2003).
[6] A. Rochefort, Appl. Magn. Reson. **67**, 11540117 (2003).
[7] M. Otani, S. Okada, and A. Oshiyama, Phys. Rev. B **68**, 125424 (2003).
[8] O. Dubay and G. Kresse, Phys. Rev. B **70**, 165424 (2004).
[9] T. Shimada, T. Okazaki, R. Taniguchi, T. Sugai, H. Shinohara, K. Suenaga, Y. Ohno, S. Mizuno, S. Kishimoto, and T. Mizutani, Appl. Phys. Lett. **81**, 4067 (2002).
[10] F. Simon, H. Kuzmany, H. Rauf, T. Pichler, J. Bernardi, H. Peterlik, L. Korecz, F. Fülöp, and A. Jánossy, Chem. Phys. Lett. **383**, 362 (2004).
[11] F. Simon *et al.*, Phys. Rev. Lett. **97**, 136801 (2006).
[12] W. Harneit, Phys. Rev. A **65**, 032322 (2002).
[13] W. Harneit, C. Meyer, A. Weidinger, D. Suter, and J. Twamley, Phys. Status Solidi B **233**, 453 (2002).
[14] T. Almeida Murphy, T. Pawlik, A. Weidinger, M. Hohne, R. Alcala, and J. M. Spaeth, Phys. Rev. Lett. **77**, 1075 (1996).
[15] S. Knorr, A. Grupp, M. Mehring, M. Waiblinger, and A. Weidinger, *Electronic Properties of Novel Materials–Molecular Nanostructures*, AIP Conf. Proc. No. 544, edited by H. Kuzmany, S. Roth, M. Mehring, and J. Fink (AIP, New York, 2000), p. 191.
[16] M. Waiblinger, K. Lips, W. Harneit, A. Weidinger, E. Dietel, and A. Hirsch, Phys. Rev. B **64**, 159901 (2001).
[17] M. Yudasaka, K. Ajima, K. Suenaga, T. Ichihashi, A. Hashimoto, and S. Iijima, Chem. Phys. Lett. **380**, 42 (2003).
[18] N. Weiden, H. Käß, and K. P. Dinse, J. Phys. Chem. B **103**, 9826 (1999).
[19] B. Corzilius, A. Gembus, K.-P. Dinse, F. Simon, and H. Kuzmany, *Electronic Properties of Novel Nanostructures*, AIP Conf. Proc. No. 786, edited by H. Kuzmany, J. Fink, M. Mehring, and S. Roth (AIP, New York, 2005), p. 291.
[20] F. Simon, C. Kramberger, R. Pfeiffer, H. Kuzmany, V. Zólyomi, J. Kürti, P. M. Singer, and H. Alloul, Phys. Rev. Lett. **95**, 017401 (2005).
[21] T. Pichler, H. Kuzmany, H. Kataura, and Y. Achiba, Phys. Rev. Lett. **87**, 267401 (2001).

[22] K. Hirahara, S. Bandow, K. Suenaga, H. Kato, T. Okazaki, H. Shinohara, and S. Iijima, Phys. Rev. B **64**, 115420 (2001).
[23] P. A. Heiney, J. E. Fischer, A. R. McGhie, W. J. Romanow, A. M. Denenstein, J. P. McCauley, A. B. Smith, and D. E. Cox, Phys. Rev. Lett. **66**, 2911 (1991).
[24] Y. Iwasa *et al.*, Science **264**, 1570 (1994).
[25] C. P. Slichter, *Principles of Magnetic Resonance*, 3rd ed. (Springer-Verlag, New York, 1989).
[26] A. M. Portis, Phys. Rev. **91**, 1071 (1953).
[27] C. P. Poole, *Electron Spin Resonance*, 3rd ed. (Wiley, New York, 1983), p. 198.
[28] A. Abragam, *Principles of Nuclear Magnetism* (Oxford University Press, Oxford, England, 1961).
[29] B. Corzilius, K.-P. Dinse, and K. Hata, Phys. Chem. Chem. Phys. **9**, 6063 (2007).